JCI insight

TIGIT signaling restores suppressor function of Th1 Tregs

Liliana E. Lucca, … , Margarita Dominguez-Villar, David A. Hafler

JCI Insight. 2019;4(3):e124427. https://doi.org/10.1172/jci.insight.124427.

Research Article Immunology

Th1 Tregs are characterized by the acquisition of proinflammatory cytokine secretion and reduced suppressor activity. Th1 Tregs are found at increased frequency in autoimmune diseases, including type 1 diabetes and multiple sclerosis (MS). We have previously reported that in vitro stimulation with IL-12 recapitulates the functional and molecular features of MS-associated Th1 Tregs, revealing a central role for hyperactivation of the Akt pathway in their induction. TIGIT is a newly identified coinhibitory receptor that marks Tregs that specifically control Th1 and Th17 responses. Here, we report that signaling through TIGIT counteracts the action of IL-12 in inducing the Th1 program. Specifically, TIGIT signaling represses production of IFN-γ and T-bet expression and restores suppressor function in Tregs treated with IL-12. FoxO1 functional inhibition abolishes the protective effect of TIGIT, indicating that TIGIT signaling promotes FoxO1 nuclear localization. Consistent with this observation, signaling through TIGIT leads to a rapid suppression of Akt function and FoxO1 phosphorylation. Finally, TIGIT stimulation reduces the production of IFN-γ and corrects the suppressor defect of Tregs from patients with MS. Our results indicate an important role for TIGIT in controlling the functional stability of Tregs through repression of Akt, suggesting that the TIGIT pathway could be targeted for immunomodulatory therapies in human autoimmune disorders.

Find the latest version:

http://jci.me/124427/pdf

JCI insight

RESEARCH ARTICLE

TIGIT signaling restores suppressor function of Th1 Tregs

Liliana E. Lucca,[1] Pierre-Paul Axisa,[1] Emily R. Singer,[1] Neal M. Nolan,[1] Margarita Dominguez-Villar,[1] and David A. Hafler[1,2]

[1]Departments of Neurology and Immunobiology, Yale School of Medicine, New Haven, Connecticut, USA. [2]Broad Institute of MIT and Harvard, Cambridge, Massachusetts, USA.

Th1 Tregs are characterized by the acquisition of proinflammatory cytokine secretion and reduced suppressor activity. Th1 Tregs are found at increased frequency in autoimmune diseases, including type 1 diabetes and multiple sclerosis (MS). We have previously reported that in vitro stimulation with IL-12 recapitulates the functional and molecular features of MS-associated Th1 Tregs, revealing a central role for hyperactivation of the Akt pathway in their induction. TIGIT is a newly identified coinhibitory receptor that marks Tregs that specifically control Th1 and Th17 responses. Here, we report that signaling through TIGIT counteracts the action of IL-12 in inducing the Th1 program. Specifically, TIGIT signaling represses production of IFN-γ and T-bet expression and restores suppressor function in Tregs treated with IL-12. FoxO1 functional inhibition abolishes the protective effect of TIGIT, indicating that TIGIT signaling promotes FoxO1 nuclear localization. Consistent with this observation, signaling through TIGIT leads to a rapid suppression of Akt function and FoxO1 phosphorylation. Finally, TIGIT stimulation reduces the production of IFN-γ and corrects the suppressor defect of Tregs from patients with MS. Our results indicate an important role for TIGIT in controlling the functional stability of Tregs through repression of Akt, suggesting that the TIGIT pathway could be targeted for immunomodulatory therapies in human autoimmune disorders.

Introduction

Tregs play a central role in the maintenance of immune tolerance, as evidenced by the multisystem autoimmune disease found in patients lacking *Foxp3*, the master regulator of Treg differentiation (1). Using in vitro assays based on in vivo experiments in rodents, Tregs have also been found to be functionally defective in a number of human autoimmune diseases (2, 3). It has been shown more recently that Tregs may adapt their function to the nature of the immune response and adopt the expression of the master transcription factor of the T effector cell (Teff) population that they suppress. Specifically, Tregs upregulate STAT3 to control pathogenic Th17 responses (4), IRF4 for the suppression of Th2 Teffs (5), and T-bet in type 1 inflammation (6). Moreover, the partial cooption of an inflammatory effector program enables Tregs to colocalize with Teffs. For example, the expression of CXCR3 by Tregs, controlled by T-bet (6), allows Tregs to migrate to sites of Th1 inflammation and thus regulate CXCR3$^+$ Th1 Teffs.

Under physiologic conditions, although Tregs may express effector-related transcription factors, they generally do not produce proinflammatory cytokines (7). However, in a number of pathologic conditions, Tregs secrete IFN-γ in association with loss of in vitro and in vivo suppressor function. We and others have reported increased frequency of IFN-γ$^+$ Tregs in autoimmune conditions such as relapsing-remitting multiple sclerosis (RR-MS) (8), type 1 diabetes (9), autoimmune hepatitis in recipients of liver transplant (10), and inflammatory bowel disease (11). Moreover, this Th1 phenotype can be recapitulated in vitro by addition of IL-12 over the course of a T cell receptor–driven stimulation (8, 12) or with conditions of high NaCl (13, 14). In patients with RR-MS, production of IFN-γ by Tregs was associated with a marked reduction in their ability to suppress Teff proliferation ex vivo compared with healthy donors. Further, blocking the autocrine/paracrine signaling of IFN-γ with an anti–IFN-γ antibody partially restored Treg suppressor function (8). These findings suggest that specific inhibition of Treg secretion of IFN-γ may have clinical utility in the treatment of human autoimmune diseases.

We have recently reported that IL-12–induced dysfunctional human Th1 Treg generation is regulated by the PI3K/Akt/FoxO1 pathway (15). Treg stimulation with IL-12 phosphorylates Akt and subsequently

Authorship note: MDV and DAH contributed equally to this work.

Conflict of interest: We have received funding from Bristol-Myers Squibb to investigate TIGIT and other costimulatory pathways in patients with brain tumors. DAH is a consultant for Compass Therapeutics, EMD Serono, Novartis Pharmaceuticals, Sanofi Genzyme, and Versant Ventures. He is also a reviewer for JDRF and a member of the scientific advisory boards of Genentech and Proclara Biosciences.

License: This work is licensed under the Creative Commons Attribution 4.0 International License.

Submitted: August 24, 2018
Accepted: January 3, 2019
Published: February 7, 2019

Reference information:
JCI Insight. 2019;4(3):e124427.
https://doi.org/10.1172/jci.insight.124427.

FoxO1, leading to its exclusion from the nucleus. Consistent with this observation, Th1 Tregs display a signature of downregulated FoxO1 transcriptional targets and activation of the PI3K/Akt/FoxO1 pathway, indicating that FoxO1 phosphorylation is both necessary and sufficient to induce Th1 Tregs. Moreover, treatment with a FoxO1 inhibitor results in increased frequency of IFN-γ$^+$ Tregs, even in the absence of IL-12, while PI3K and Akt inhibitors repressed IFN-γ and restored function in IL-12–treated Tregs. These results, together with the observation that human Th1 Tregs can be induced with IL-12 without prior IFN-γ sensitization, suggest that prevention of Th1 reprogramming might be better controlled by negative regulators of Akt than delayed activation of STAT4, as demonstrated in rodent Tregs (8).

T cell immunoglobulin with ITIM domain (TIGIT) is a recently identified coinhibitory receptor highly expressed by Tregs (16, 17). TIGIT outcompetes the costimulatory receptor CD226 for binding to CD155, for which it has a 100-fold higher affinity (16). By engaging CD155 on dendritic cells, TIGIT inhibits IL-12 and induces secretion of IL-10 in *trans* (16). Moreover, TIGIT disrupts CD226 dimerization and signaling in *cis* (18), displaying a T cell–intrinsic function that results in suppression of Th1 and Th17 responses (18, 19). While proximal signaling of TIGIT has not been examined in primary T cells, studies in transfected Jurkat cells and primary NK cells revealed that, upon TIGIT engagement by CD155, the PI3K pathway repressor SHIP-1 is recruited to the cytoplasmic tail of TIGIT. Importantly, the formation of this complex is required for TIGIT-mediated inhibition of cytotoxicity (20). Additionally, we and others have reported that TIGIT$^+$ Tregs are more potent than TIGIT$^-$ Tregs in suppressing Th1 and Th17 responses, while sparing the function of Th2 Teffs (21). Consistent with this observation, transcriptional analysis revealed that TIGIT$^+$ Tregs express higher levels of CXCR3 and other genes that define Th1-suppressing CXCR3$^+$ Tregs (6, 21). Thus, TIGIT expression is required for optimal suppression of Th1 inflammation. In this regard, it has been show that Tregs that are more prone to acquire expression of IFN-γ in vitro have an increased expression of CD226 and a lower expression of TIGIT (22). These data are of interest in relationship to human autoimmune diseases, as genetic variants in CD226 are associated with risk of developing type 1 diabetes and multiple sclerosis (MS) (23, 24). These observations led us to hypothesize that Tregs use TIGIT signaling to enhance suppression of Th1 Teff responses without undergoing detrimental Th1 reprogramming.

Here, we examined the role of TIGIT signaling in the induction and maintenance of human Th1 Tregs. We demonstrate that TIGIT stimulation using a CD155 Fc chimera protein (Fc-CD155) inhibits the induction of IFN-γ expression induced ex vivo by IL-12 in primary human Tregs from healthy donors. Moreover, this inhibition of IL-12–induced IFN-γ secretion corrects the loss of in vitro suppressor function. TIGIT stimulation directly represses phosphorylation of Akt and FoxO1, while inhibition of either FoxO1 or SHIP-1 abolishes the effect of TIGIT stimulation in the conversion of Tregs to the Th1 program. These data demonstrate that TIGIT functionally controls the Akt pathway via SHIP1. Finally, IFN-γ–secreting Tregs isolated ex vivo from the circulation of patients with MS that have lost in vitro suppressor function have a gain in function with loss of IFN-γ secretion after TIGIT stimulation. These data suggest that direct stimulation of TIGIT can correct defects in autoimmune Tregs.

Results

As TIGIT$^-$CD226$^+$ Tregs lose suppressor activity and acquire the capacity to secrete IFN-γ (22), we explored the relationship among TIGIT, CD226, and IFN-γ under Th1 conditions (Figure 1). The majority of Tregs from healthy donors expressed TIGIT ex vivo (Figure 1A), and TIGIT expression was maintained after stimulation with αCD3 and αCD28 in the presence of IL-2 and IL-12 for 4 days (Figure 1B). When gating Tregs into subpopulations based on the expression of TIGIT and CD226, we observed that, as previously reported, the majority of IFN-γ$^+$ Tregs were in either TIGIT$^+$CD226$^+$ or TIGIT$^-$CD226$^+$ populations (Figure 1, B and C). While CD226 identified IFN-γ$^+$ Tregs, a significant proportion of IFN-γ$^+$ Tregs expressed TIGIT, leading to the hypothesis that IFN-γ production can be modulated in Tregs by TIGIT stimulation. To examine the role of TIGIT in Treg IFN-γ production, Tregs were activated with αCD3, αCD28, and IL-2 with or without IL-12, and TIGIT was stimulated with Fc-CD155. This led to a significant reduction of the frequency of IFN-γ$^+$ Tregs after 3 days of culture (Figure 1E and Supplemental Figure 1A; supplemental material available online with this article; https://doi.org/10.1172/jci.insight.124427DS1). Nevertheless, since CD155 can bind both CD226 and TIGIT, this effect could be due to signaling downstream of either receptor. In order to identify which receptor is driving restriction of IFN-γ expression, we pursued two approaches. Initially, we stimulated Tregs to induce the Th1 phenotype in the presence of a previously validated agonistic αTIGIT antibody (19); this treatment recapitulated the effect of Fc-CD155 in decreas-

ing the frequency of IFN-γ$^+$ Tregs (Figure 1, D and F). Second, we used CRISPR/Cas9 to delete *CD226* from sorted Tregs prior to activation with αCD3, αCD28, IL-2, and IL-12 and stimulation with Fc-CD155 or isotype control (25). While the CRISPR/Cas9 experimental method required prior in vitro expansion of Tregs, Fc-CD155 stimulation of TIGIT reduced the frequency of IFN-γ$^+$ Tregs to a similar extent as in ex vivo Tregs (Figure 1, G and I). After confirming the efficacy of CD226 knockdown at the protein level by flow cytometry (Figure 1, G and H), we compared the effect of Fc-CD155 stimulation in CD226$^{-/-}$ and control Tregs; in both cases the frequency of IFN-γ$^+$ Tregs was significantly reduced (Figure 1, I and J). These data are consistent with the higher affinity of CD155 for TIGIT rather than CD226 and suggest that the effects of Fc-CD155 on the inhibition of Th1 Tregs are primarily mediated by TIGIT.

We have previously reported that activation of Tregs with IL-2 and IL-12 decreased functional suppression of Teff proliferation. In order to determine whether suppression of IFN-γ by TIGIT engagement corrects loss of suppression, we preactivated Tregs in IL-2 or IL-2 and IL-12 conditions and stimulated TIGIT via Fc-CD155. After 4 days, we examined the suppressor activity of preactivated Tregs by coculturing them with Teffs and assessing Teff proliferation. We observed that IL-2 and IL-12 pretreatment resulted in decreased suppression, while TIGIT stimulation led to a gain of Treg suppressor function (Figure 2, A–C). At the end of the coculture, consistent with what has previously been reported (15), IFN-γ production by IL-2– and IL-12–treated Tregs was inversely correlated with suppressor function (Supplemental Figure 1, B and C). Moreover, we observed that Tregs produced less IFN-γ if they had received Fc-CD155 stimulation together with the IL-2 and IL-12 pretreatment (Figure 2D). Finally, we observed a reduction in the overall amount of IFN-γ secreted in the coculture under IL-2 and IL-12 with Fc-CD155 conditions (Figure 2E), which, at the 1:16 Treg/Teff ratio, is likely to originate predominantly from the Teff population. These results indicate that TIGIT stimulation inhibits Treg acquisition of a Th1 phenotype in type 1 inflammation.

Th1 reprogramming of Tregs requires activation of the PI3K pathway with phosphorylation of FoxO1, causing its exclusion from the nucleus that leads to unrepressed T-bet and IFN-γ transcription (26). Since it has been reported that TIGIT recruits the phosphatase SHIP-1 (20), a repressor of Akt signaling through degradation of PIP_3, we reasoned that TIGIT signaling could limit T-bet expression through inhibition of Akt activity. To test this hypothesis, we stimulated sorted Tregs with IL-12, αCD3 and αCD28, and Fc-CD155. As previously reported (15), stimulation with αCD3 and αCD28 coupled with IL-12 resulted in detectable phosphorylation of Akt at threonine 308 (Figure 3, A and B) and slightly delayed phosphorylation of FoxO1 at serine 256 (Figure 3, A and C), an Akt-specific phosphorylation site. We observed repressed Akt function, as measured by phosphorylation, at those residues with Fc-CD155 stimulation (Figure 3, A–C). Phosphorylation of FoxO1 at serine 256 prevents its nuclear translocation and transcriptional activity (27). Thus, we sought to confirm that Fc-CD155 stimulation results in FoxO1 nuclear localization in Tregs. To this end, we sorted Tregs and activated them with αCD3, αCD28, and IL-12 for 16 hours, a time point at which we had previously detected induction of FoxO1 phosphorylation by IL-12 (15). The analysis of the nuclear versus cytoplasmic localization of FoxO1 by confocal microscopy, based on the overlap between DAPI and FoxO1 fluorescence, showed that Treg activation in vitro results in FoxO1 exclusion from the nucleus (Figure 3, D and E). When Fc-CD155 was added to Tregs stimulated for 18 hours, we observed a significant increase in the proportion of nuclear FoxO1 (Figure 3, D and F). Thus, Fc-CD155 represses Akt activation and results in greater availability of FoxO1 in the nucleus. In order to assess whether this led to reduced T-bet induction, we measured T-bet expression and FoxO1 phosphorylation by flow cytometry in Tregs activated under Th1 conditions in the presence of Fc-CD155 stimulation over 4 days. We observed that, indeed, Fc-CD155 treatment decreased the frequency of Tregs that express T-bet and the phosphorylated form of FoxO1 (Figure 4, A and B).

We previously demonstrated that inhibition of FoxO1 with AS1842856 was sufficient to induce Th1 reprogramming in Tregs (15). As we hypothesize that TIGIT blocks Th1 reprogramming by preventing FoxO1 phosphorylation with reduced FoxO1 exclusion from the nucleus, we reasoned that inhibiting FoxO1 would block the effect of Fc-CD155 stimulation. Indeed, when we induced Th1 Tregs with concomitant TIGIT triggering through Fc-CD155 and FoxO1 inhibition, we did not observe a significant reduction in the frequency of IFN-γ$^+$ Tregs (Figure 4, C–E), suggesting that nuclear localization of FoxO1 is required for TIGIT repression of IFN-γ.

We then determined whether SHIP-1 is the phosphatase used by TIGIT to repress the Akt/FoxO1/T-bet/IFN-γ axis in Tregs. We initially determined whether SHIP-1 is recruited to the immunological synapse during αCD3, αCD28, and IL-12 stimulation, which can be assessed by quantifying SHIP-1 phosphorylation at tyrosine 1021 that is required for SHIP-1 docking (28). We observed a rapid phosphorylation of tyrosine

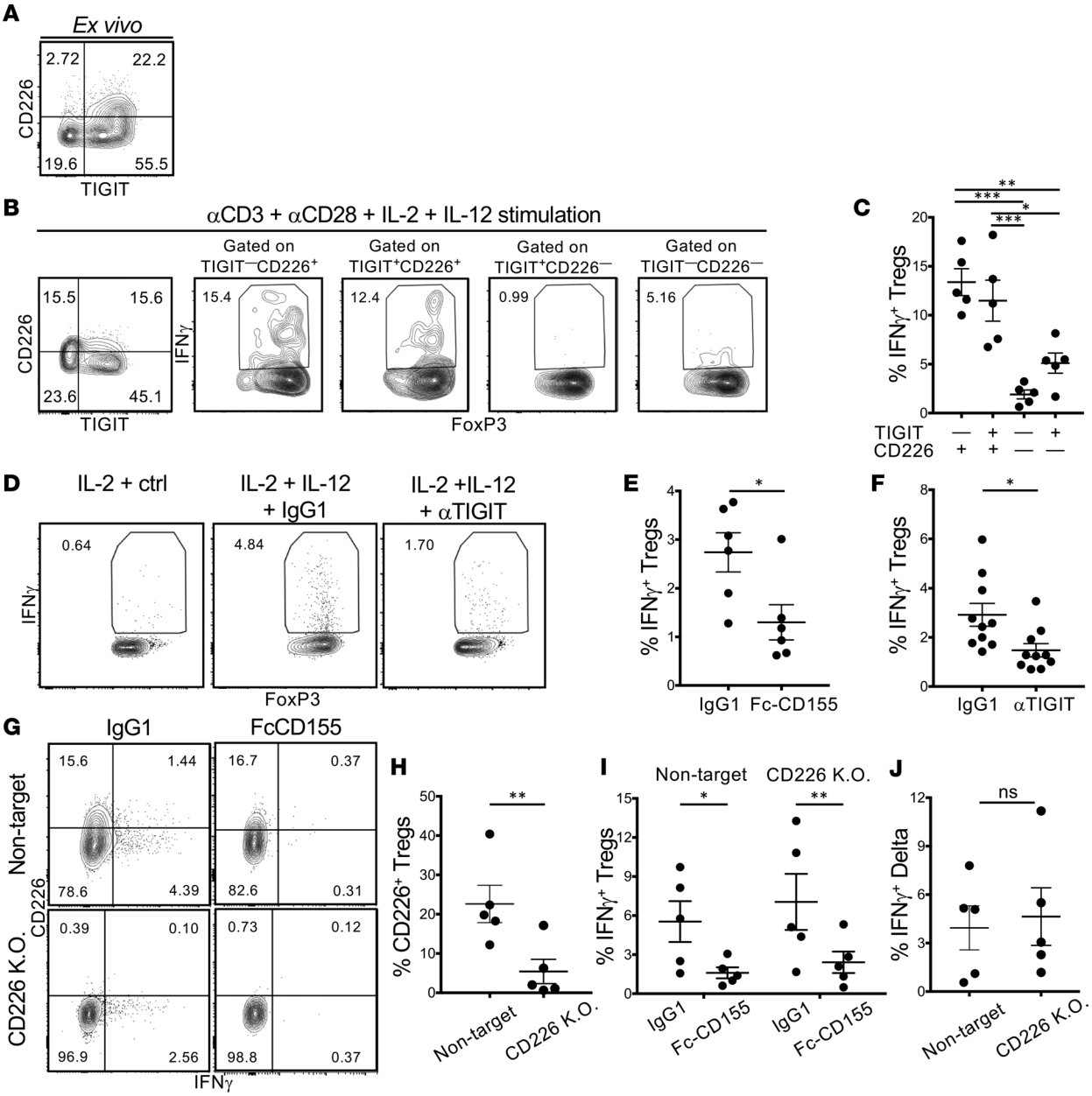

Figure 1. TIGIT stimulation suppresses the induction of IFN-γ⁺ Tregs in Th1 conditions. (**A**) Representative expression of TIGIT and CD226 by Tregs ex vivo. (**B** and **C**) $CD4^+CD25^{hi}CD127^{lo}$ Tregs were stimulated for 4 days with αCD3+αCD28 and IL-2+IL-12, and the frequency of IFN-γ⁺ Tregs among the 4 TIGIT versus CD226 gates was measured. A representative experiment (**B**) and summary of 5 donors are shown (**C**, 1-way ANOVA with Tukey's multiple comparison correction). (**D–F**) Tregs were activated as in **B**, with or without TIGIT stimulation. A representative experiment (**D**) and quantification of the frequency of IFN-γ⁺ Tregs induced in IL-2+IL-12 conditions with or without agonistic αTIGIT antibody (**F**, paired *t* test, $P = 0.027$) or Fc-CD155 are shown (**E**, paired *t* test, $P = 0.0118$). (**G–L**) Expanded Tregs were electroporated in the presence of Cas9 gRNAs RNP complexes and subsequently stimulated as in **B**. (**G**) Representative staining for IFN-γ and CD226. Quantification of the reduction in protein expression of CD226 by CRISPR knockdown (**H**, ratio paired *t* test, $P = 0.0168$); quantification of IFN-γ induction in IL-2+IL-12 conditions with or without FcCD155 in Tregs treated with a CD226 or nontarget guide RNA (**I**, ratio-paired *t* test, $P = 0.0252$ for the nontarget condition and $P = 0.0075$ for the CD226 K.O. condition); direct comparison of the FcCD155 effect on IFN-γ in Tregs treated with a CD226 or nontarget gRNA (**J**, paired *t* test, $P = 0.7158$). $^*P < 0.05$, $^{**}P < 0.005$, $^{***}P < 0.0005$.

1021 over the first minute of stimulation, compatible with the early effect of TIGIT stimulation in repressing Akt phosphorylation. Importantly, above-background phosphorylation of SHIP-1 was detectable regardless of TIGIT stimulation, which is consistent with the observation that this residue is the target of Syk and Lyn, whose function is not known to be controlled by TIGIT (29) (Supplemental Figure 2, A and B).

To assess whether the activity of SHIP-1 is necessary for TIGIT repression of Th1 conversion, we activated Tregs with αCD3, αCD28, IL-2, and IL-12 and compared the magnitude of the Fc-CD155 effect in the presence

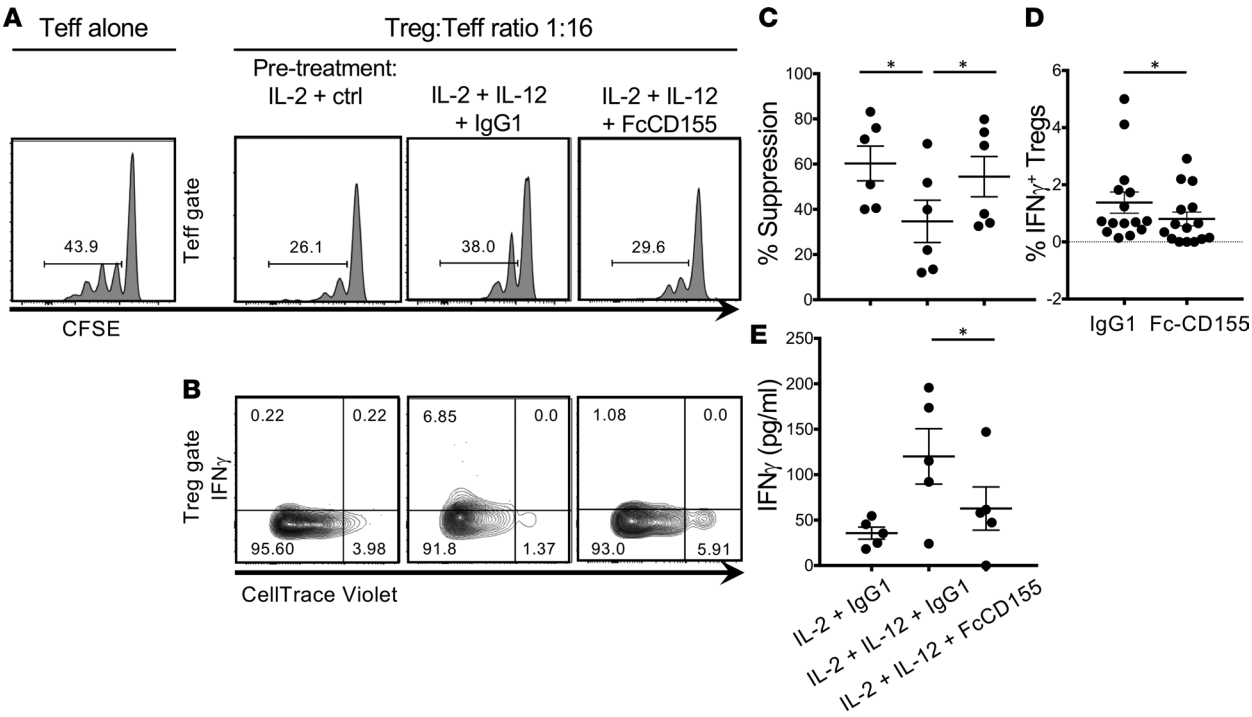

Figure 2. TIGIT stimulation restores suppression to Tregs treated in Th1 conditions. Tregs were stimulated for 4 days with αCD3+αCD28 and the following treatments: IL-2+IgG1 ctrl, IL-2+IL-12+IgG1 ctrl, and IL-2+IL-12+FcCD155. After 4 days, Tregs were washed and cocultured with Teffs in a suppression assay. A representative experiment displaying the proliferation of Teffs at 1:16 Treg/Teff ratio (**A**) and the proliferation and IFN-γ production of the Tregs (**B**). (**C**) Quantification of the suppression activity (paired *t* test with Bonferroni's correction for multiple comparisons, IL-2 +IgG1 vs. IL-2+IL-12 +IgG1, $P = 0.0068$; IL-2+IL-12+IgG1 vs. IL-2+IL-12+FcCD155, $P = 0.0036$). (**D**) Comparison of the frequency of IFN-γ$^+$ Tregs at ratios of 1:1 to 1:16 between the IL-2+IL-12+IgG1 ctrl and Il-2+IL-12+FcCD155 treatment (each dot represents a Treg/Teff ratio; paired *t* test, $P = 0.0195$). (**E**) Quantification of the secretion of IFN-γ in the supernatant of cocultures of Tregs and Teffs at the 1:16 ratio from 4 donors (paired *t* test with Bonferroni's correction for multiple comparisons, $P = 0.0654$ for the IL-2+IgG1 vs. IL-2+IL-12+IgG1 condition and $P = 0.0412$ for the IL-2+IL-12+IgG1 and IL-2+IL-12+FcCD155 condition). *$P < 0.05$.

of a SHIP-1 inhibitor or vehicle. We observed that inhibition of SHIP-1 reduces the capacity of TIGIT to inhibit the generation of IFN-γ$^+$ Tregs (Figure 4, F–H). Similar results were also obtained when triggering TIGIT with the αTIGIT agonistic antibody (Supplemental Figure 2, C and D). Taken together, these results suggest that SHIP-1 is a nonredundant partner of TIGIT in controlling the Th1 reprogramming of Tregs.

Finally, given that dysfunctional Tregs secreting IFN-γ are a hallmark of immune dysfunction in MS, we explored whether TIGIT stimulation corrected this defect in immune regulation. Initially, we assessed whether the frequency of TIGIT and CD226 was similar in new-onset RR-MS patients and healthy donors and observed that patients with RR-MS displayed an increased frequency of circulating CD226$^+$ Tregs compared with that of healthy donors (Figure 5, A and B). This difference was reduced after 4 days of stimulation with αCD3 and αCD28 (Figure 5, C and D).

Since we did not observe changes in TIGIT at the protein level in patients with RR-MS as compared with healthy individuals, we sought to confirm that the TIGIT pathway is functional in patients with the disease, as previously reported for memory CD4 Teffs (19). Stimulation of Tregs with Fc-CD155 revealed that, in both IL-2 and IL-2 and IL-12 conditions, the frequency of IFN-γ$^+$ Tregs (Figure 5, E and G) and the expression of T-bet (Figure 5, E and H) could be repressed by TIGIT signaling. A similar effect was observed for CD226 (Figure 5F), further stressing that CD226 expression is a marker of IFN-γ production. Since stimulation of Tregs with IL-12 models the functional impairment of Tregs in RR-MS (8), we hypothesized that TIGIT signaling would restore the suppressor function of ex vivo Tregs from RR-MS patients. We preactivated Tregs from new-onset RR-MS patients and healthy donors with αCD3, αCD28, and IL-2 for 4 days; stimulated TIGIT via Fc-CD155; and cocultured the Tregs with healthy donor Teffs. Indeed, in patients displaying a lower suppressor activity compared with that of the healthy donors (5 of 6 subjects), pretreatment with Fc-CD155 restored the capacity of Tregs to inhibit Teff proliferation (Figure 5, I and J). Thus, these observations indicate that TIGIT stimulation restores the functional impairment acquired in vivo by Tregs in patients with RR-MS.

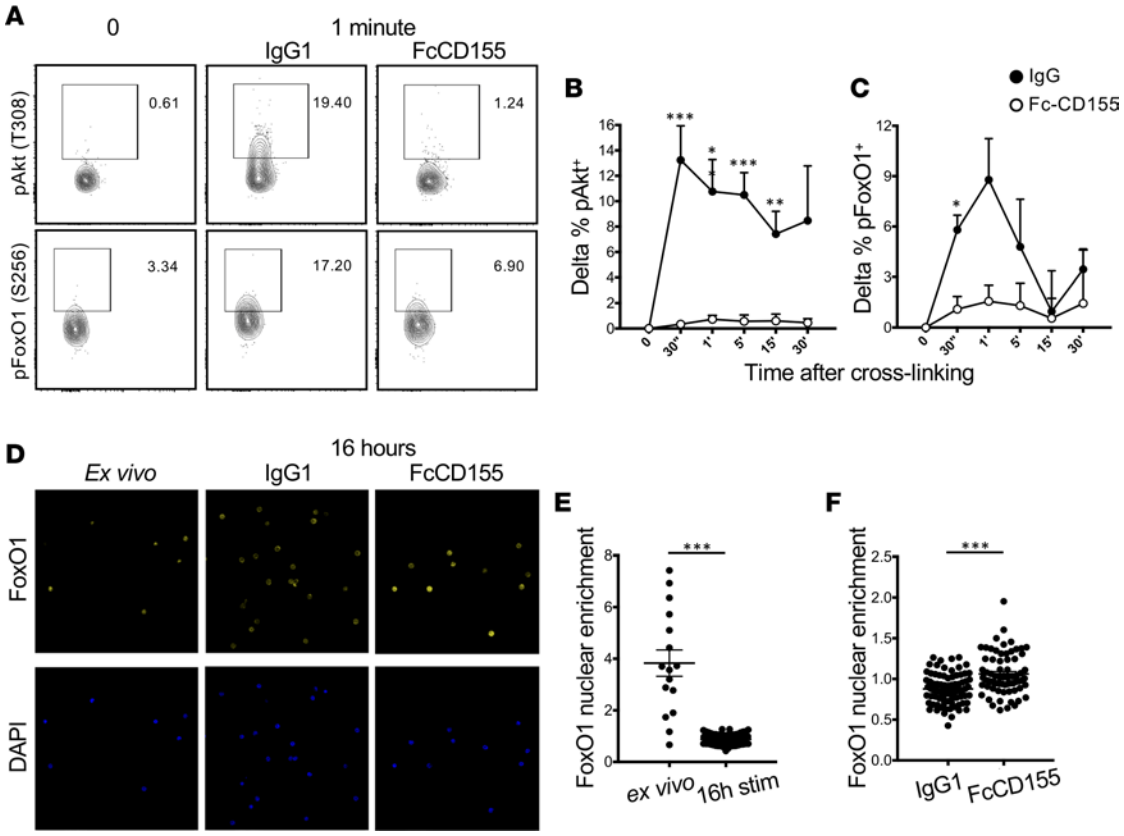

Figure 3. TIGIT stimulation suppresses the Akt/FoxO1 pathway. (**A**–**C**) Tregs stimulated for the indicated times with αCD3+αCD28, IL-12, Fc-CD155, or isotype control. One representative experiment (**A**) and quantification of the delta between the indicated time points and the time 0 condition are shown (**B**, $n = 7$ for pAkt, and **C**, $n = 5$ for pFoxO1, paired t test with Bonferroni's correction for multiple comparisons). (**D**–**F**) Sorted Tregs were rested in serum-free media for 2 hours and then fixed (ex vivo) or stimulated with αCD3+αCD28, IL-12, FcCD155, or isotype control overnight (16 hours). One representative experiment showing immunofluorescent staining for DAPI and FoxO1 (original magnification, ×63) (**D**) and quantification of the nuclear enrichment of FoxO1 for 2 donors (**E** and **F**, 2 outliers were removed [ROUT Q = 10%], unpaired t test, $P < 0.0001$; ex vivo = 16 cells, 16hstim = 80 cells, IgG1 = 80 cells, FcCD155 = 71 cells). $^*P < 0.05$, $^{**}P < 0.005$, $^{***}P < 0.0005$.

Discussion

Th1 Tregs with loss of in vitro suppressor function are observed in a number of autoimmune diseases; these Th1 Tregs are thought, in part, to mediate loss of immune regulation, allowing activation of autoreactive T cells. Understanding the mechanisms associated with loss of Treg function might allow novel therapeutic approaches to correct immune regulatory defects in autoimmunity. We previously demonstrated that stimulating TIGIT induces the secretion of Fgl-2, a cytokine that can modulate APC function toward an antiinflammatory profile (21). Here, we report that stimulation of TIGIT, a coinhibitory receptor identifying Tregs that control Th1 and Th17 responses, prevents proinflammatory reprogramming of Tregs to Th1 Tregs and preserves their suppressor function. Specifically, TIGIT signaling through Fc-CD155 repressed IFN-γ and T-bet expression and restored suppressor function in Tregs treated with IL-12. Stimulation of the TIGIT pathway repressed PI3K signaling while promoting rapid suppression of Akt function accompanied by FoxO1 phosphorylation with nuclear localization. Finally, TIGIT stimulation reduced IFN-γ expression and corrected the suppressor defect of Tregs from patients with MS. Our results indicate an important role for TIGIT in controlling the functional stability of Tregs through repression of Akt, suggesting that the TIGIT pathway could be targeted for immunomodulatory therapies in human autoimmune disorders.

Controlling the activity of the PI3K pathway upon activation is crucial for maintenance of the Treg lineage. In this regard, we observed that TIGIT represses PI3K signaling. Tregs lacking the phosphatase PTEN, which dephosphorylates the second messenger PIP_3, ultimately lose suppressor function and stable FoxP3 expression (30). Similar scenarios resulting in unstable Tregs unable to restrain inflammatory responses in vivo have been reported when hyperactivating the PI3K pathway, either by disrupting the

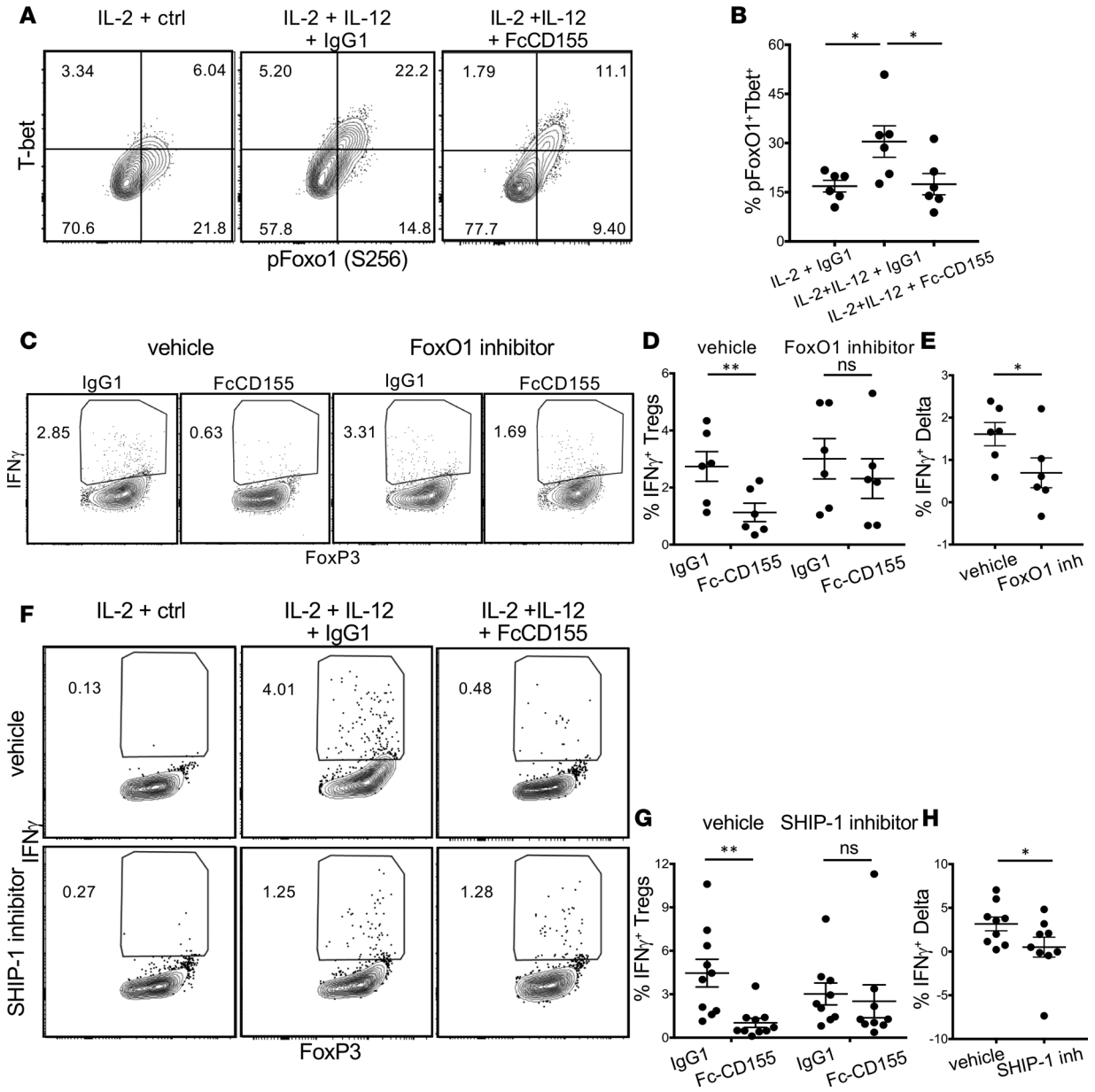

Figure 4. Suppression of IFN-γ by TIGIT stimulation is dependent on FoxO1 and SHIP-1 function. (**A** and **B**) Tregs were stimulated for 4 days with αCD3+αCD28, IL-2, or IL-2+IL-12 with or without Fc-CD155. One representative experiment (**A**) and quantification of the frequency of T-bet$^+$pFoxO1$^+$ Tregs for 6 donors (**B**, paired *t* test with Bonferroni's correction for multiple comparisons, IL-2+IgG1 vs. IL-2+IL-12+IgG1, $P = 0.027$; IL-2+IL-12+IgG1 vs. IL-2+IL-12+FcCD155, $P = 0.044$). (**C**–**E**) Tregs were stimulated for 4 days with αCD3+αCD28, IL-2, or IL-2+IL-12 with or without Fc-CD155 and in the presence of FoxO1 inhibitor (AS1842856 25nM) or vehicle (DMSO). One representative experiment (**C**) and summary for 6 donors are shown (**D**, paired *t* test, $P = 0.0021$ for the vehicle condition and $P = 0.1062$ for the FoxO1 inhibitor condition; **E**, paired *t* test, $P = 0.0325$). (**F**–**H**) Tregs were stimulated for 4 days with αCD3+αCD28, IL-2, or IL-2+IL-12 with or without Fc-CD155 and in the presence of a SHIP-1 inhibitor (3AC 1 mM) or vehicle (EtOH). One representative experiment (**F**) and quantification for 8 donors (**G**, paired *t* test, $P = 0.0036$ for the *vehicle* condition, $P = 0.6695$ for the *SHIP-1 inhibitor* condition; **H**, paired *t* test, $P = 0.0482$). $^*P < 0.05$, $^{**}P < 0.005$.

Semaphorin4a/Neuropilin1 axis (31) or by deleting FoxO1 and FoxO3a (26). Thus, TIGIT signaling preserves functional and lineage stability of Tregs.

TIGIT signaling by Fc-CD155 promotes the ability of Tregs to suppress Teff proliferation. This effect was only seen in conditions in which suppressor function is destabilized, as in the case of treatment with IL-12 or when Tregs were derived from RR-MS patients. Our results are consistent with those of a recent study in which Fc-CD155 was shown to enhance suppressor activity of tumor-derived Tregs through interaction with TIGIT (32) in patients with melanoma. In those experiments, CD226 signaling by Fc-CD155

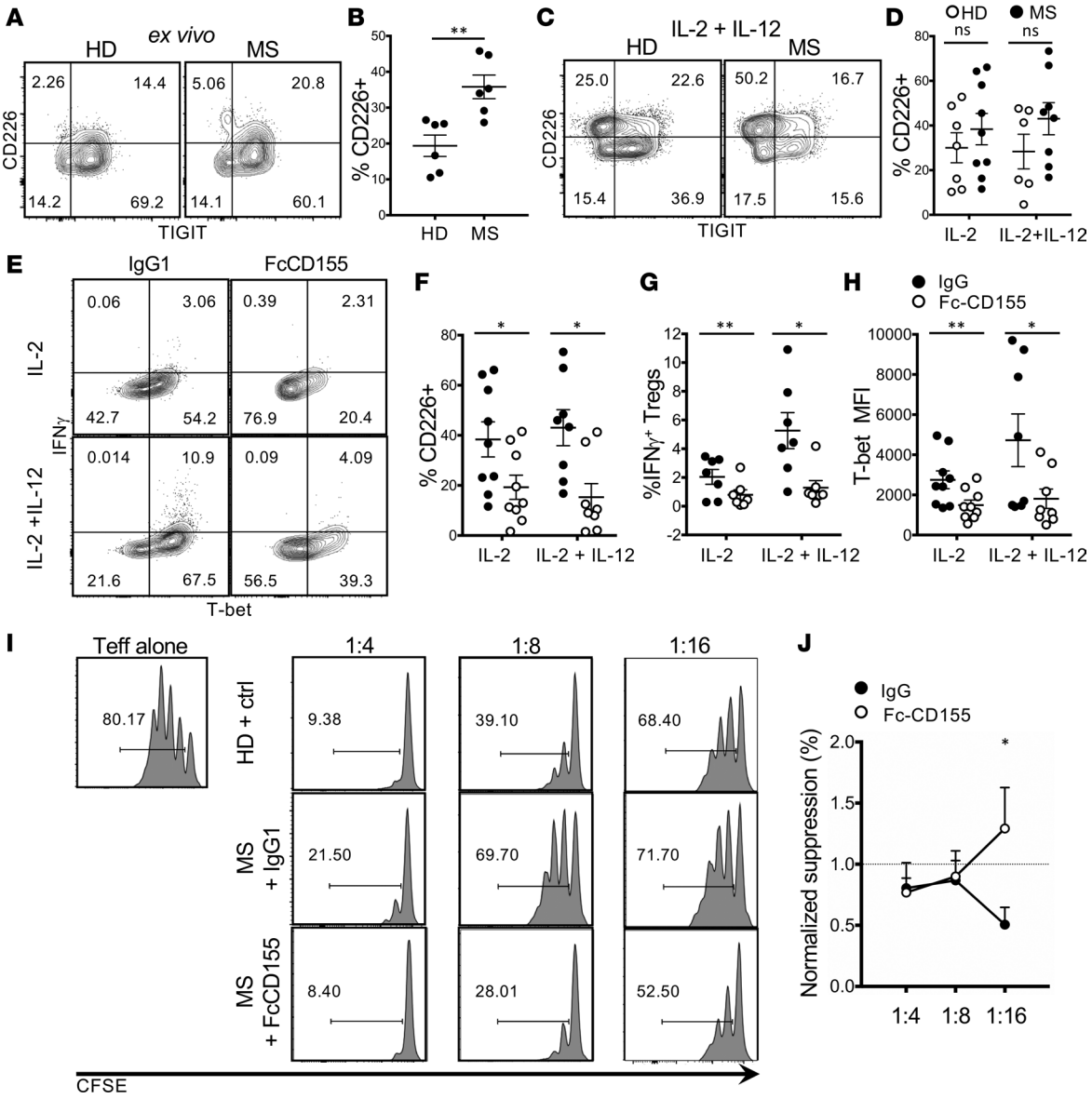

Figure 5. TIGIT stimulation suppresses IFN-γ and restores suppression in Tregs from MS patients. (**A** and **B**) Expression of TIGIT and CD226 on Tregs from new-onset untreated MS patients (MS) and healthy donors (HD). Tregs were gated as Live/CD4$^+$/CD25^{hi}/Foxp3$^+$. One representative experiment (**A**) and summary of 5 donors are shown (**B**, unpaired *t* test, $P = 0.0051$). (**C** and **D**) Expression of TIGIT and CD226 by Tregs from MS patients after 4 days of stimulation with αCD3+αCD28 and IL-2 or IL-2+IL-12. One representative experiment (**C**) and summary of 7 HD and 9 MS patients are shown (**D**, ratio paired *t* test with Bonferroni's correction for multiple comparisons, $P = 0.4094$ for the IL-2 condition and $P = 0.1795$ for the IL-2+IL-12 condition). (**E**–**H**) Expression of IFN-γ and T-bet by Tregs from MS patients activated as in **B** with or without Fc-CD155. One representative experiment (**E**) and summaries of 7–9 MS patients are shown (ratio paired *t* test with Bonferroni's correction for multiple comparisons; **F**, $P = 0.021$ for the IL-2 condition and $P = 0.0194$ for the IL-2+IL-12 condition; **G**, $P = 0.0042$ for the IL-2 condition and $P = 0.0124$ for the IL-2+IL-12 condition; **H**, $P = 0.0096$ for the IL-2 condition and $P = 0.0112$ for the IL-2+IL-12 condition). (**I** and **J**) Tregs were activated as in **B**, with or without Fc-CD155. After 4 days, Tregs were cocultured with Teffs in a suppression assay. (**I**) One representative experiment (Teff gate). (**J**) Quantification of Treg suppression normalized by the suppression of the matched HD (paired *t* test with Bonferroni's correction for multiple comparisons, $n = 5$, $P = 0.0147$). $^*P < 0.05$, $^{**}P < 0.005$.

decreased Treg function, possibly mediated by a reduction of FoxP3 expression. While we did not assess the effect of genetic deletion of *CD226* on Treg suppression, we observed similar effects of Fc-CD155 stimulation on the generation of IFN-γ$^+$ Tregs when CD226 was either expressed or knocked down through CRISPR/Cas9. It will be of interest to measure IFN-γ$^+$ in tumor-derived Tregs with CD226 and TIGIT signaling. It has been reported that CD226 triggering can enhance phosphorylation of Akt through recruitment of the PI3K regulatory subunit p85 (33, 34). Because treatment of Tregs with IL-12 also results in heightened Akt activity, it is conceivable that the effect of CD226 on Akt function would be redundant

when this pathway is already hyperactive, a scenario that would explain why an effect of CD226 is seen when Tregs are activated without IL-12 (32) but not after IL-12 stimulation. Further studies centered on CD226 signaling in Th1 Tregs are required to better understand its function in Tregs.

While both CD155 and CD112 are ligands for CD226, CD112 has a significantly greater affinity for CD226 as compared with TIGIT (16). Thus, it would be of interest to assess signaling downstream of TIGIT and CD226 in the context of stimulation with physiologically relevant combinations of CD112 and CD155. Finally, our observation that the expression of CD226 is heightened in ex vivo Tregs from RR-MS patients and repressed by Fc-CD155 stimulation, similar to what is observed with T-bet and IFN-γ, is consistent with the previously reported association between this costimulatory receptor and IFN-γ production (22).

While we demonstrated that TIGIT stimulation results in reduced phosphorylation of FoxO1 that is maintained over time, there may be other mechanisms whereby TIGIT represses the induction of Th1 programs. For example, upstream inhibition of PI3K by TIGIT results in inhibition of mTOR, and other substrates of mTOR could be involved. It is worth noting that Fgl-2 production by Tregs, which is under the control of TIGIT, was reported as a hallmark of tolerance to allografts in mice treated with the mTOR inhibitor rapamycin (35), further strengthening the connection between TIGIT signaling and PI3K signaling.

While we demonstrate that SHIP-1 is required for suppression of IFN-γ with TIGIT signaling, we paradoxically observed a modest decrease in IFN-γ^+ Tregs when inhibiting SHIP-1 without TIGIT stimulation, even though SHIP-1 was phosphorylated with T cell receptor stimulation. In contrast, IFN-γ expression after Fc-CD155 stimulation of Tregs in the presence of a SHIP-1 inhibitor resulted in a higher frequency of IFN-γ^+ Tregs in the majority of donors. We then measured the relative frequency of IFN-γ^+ Tregs with and without Fc-CD155 and observed Fc-CD155 stimulation did not significantly reduce the generation of Th1 Tregs (Figure 4H) with inhibition of SHIP-1. Thus, these data suggest that the function of SHIP-1 is nonredundant for TIGIT signaling.

It is known that there are multiple downstream consequences of SHIP-1 activity on PI3K signaling. Unlike PTEN, the enzymatic activity of SHIP-1 does not result in PIP_3 signaling termination, but instead in the generation of $PI_{(3,4)}P_2$, which retains the ability to activate Akt. The intensity of the downstream Akt activation when PIP_3 is converted to $PI_{(3,4)}P_2$ thus depends on the competition between Akt and other molecules that can bind $PI_{(3,4)}P_2$, such as the inhibitory proteins TAPP1/2 (36). While further work is required to dissect the functional specificities of $PI_{(3,4)}P_2$ and PIP_3 in human Tregs, it appears that SHIP-1 might allow finely tunable control over Akt in Tregs. In fact, notwithstanding the previously described requirement for low Akt activity for Treg functional stability, recent work has highlighted that some degree of FoxO1 exclusion from the nucleus is required for Treg homing to nonlymphoid organs and activation in tissue (37).

We and others previously showed that inactivating PTEN is sufficient to destabilize Tregs and inhibit their suppressor function (15, 30). Our data suggest that this occurs for SHIP-1 in the context of TIGIT activation. Interestingly, SHIP-1 expression is confined to hematopoietic cells, suggesting that it could be modulated pharmacologically in a more specific way. This might be of particular relevance in the context of immunotherapy for nonhematological cancers. For example, CD155 is expressed by different solid tumors (18, 32, 38, 39), suggesting that TIGIT may be triggered in the tumor microenvironment. On the other hand, loss-of-function mutations in *Pten* are often acquired during cancer progression; in this context, inhibition of PTEN might actually favor cancer growth, whereas inhibition of SHIP-1 might result in Treg destabilization without the risk of tumor cell proliferation. Indeed, a recent report describes improved antitumoral T cell immunity following administration of a SHIP-1 inhibitor (40).

As these are human systems, it is not possible to perform fate-mapping experiments, and thus it is difficult to determine whether TIGIT works by preventing the conversion of functional Tregs into Th1 Tregs or by reverting the Th1 programs of already fully committed dysfunctional IFN-γ^+ Tregs. The fact that approximately half of the IFN-γ^+ Tregs generated in IL-2 and IL-12 condition expressed TIGIT leaves open both possibilities. Nevertheless, we demonstrate that TIGIT stimulation corrects the functional Treg defect of RR-MS patients, in an experimental setting in which no exogenous IL-12 was added, suggesting that this defect was acquired in vivo. The underlying causes of the functional impairment of RR-MS Tregs are likely to involve both genetic and environmental interactions. Indeed, RR-MS–associated risk variants in *CD58* (41) and *IL2RA* (42) have been reported to alter Treg function. Interestingly, 2 RR-MS–related genetic SNPs have been identified in the TIGIT pathway: one in the *CD155* locus (43) as well as the Gly307Ser *CD226* variant (23, 24). Moreover, we have shown that environmental exposure to high-salt conditions leads to loss of Treg function associated with increases in IFN-γ expression (13). Thus, future studies are required to

understand whether insufficient engagement of TIGIT in genetically susceptible hosts under certain environmental conditions contributes to Treg proinflammatory reprogramming. Finally, recent work in the mouse model of RR-MS has shown that functional αTIGIT antibodies can modulate disease severity (44). Our results agree with these in vivo data and suggest that TIGIT stimulation could represent a viable therapeutic strategy to correct the immune regulation defects observed in RR-MS and other autoimmune diseases.

Methods

Human subjects. Peripheral blood was obtained from healthy volunteers (average age, 28.8 years; minimum, 23 years; maximum, 43 years). Peripheral blood mononuclear cells (PBMCs) were cryopreserved from 9 RR-MS patients (average age, 35.8 years; minimum, 26 years; maximum, 60 years) and 7 healthy volunteers (average age, 37 years; minimum, 27 years; maximum, 61 years). Patients had a disease duration not exceeding 5 years, were not on disease-modifying treatment, and had not received steroids for at least a year before blood collection.

Cell isolation and FACS sorting of T cell populations. PBMCs were isolated by Ficoll gradient centrifugation and used directly for downstream applications in all experiments except for those in Figure 4, where PBMCs had been cryopreserved in 90% human AB serum (Gemini Bio-Products) and 10% DMSO (MilliporeSigma) in liquid nitrogen. Total CD4 T cells were obtained by negative selection using the Easysep $CD4^+$ T cell enrichment kit (StemCell Technologies, 19052) and stained with antibodies for CD4 (clone RPA-T4), CD25 (clone 2A3), and CD127 (clone hIL-7R-M21, all from BD Biosciences). Tregs were defined as the top 2%–4% of $CD4^+CD25^{hi}CD127^{lo}$ cells and Teffs were defined as $CD4^+CD25^{lo/int}CD127^+$.

Induction of Th1 Tregs. Sorted Tregs were cultured for 4 days in standard culture conditions in RPMI 1640 media (Gibco) supplemented with 2 nM L-glutamine, 5 mM HEPES, 100 U/μg/ml penicillin/streptomycin (Biowhittaker), 0.5 mM sodium pyruvate, 0.05 mM nonessential amino acids (Life Technologies; complete RPMI), and 5% GemCell human AB serum (GemBio). Tregs were stimulated with anti-human CD3 (clone UCHT1, BD Biosciences) and anti-human CD28 (clone 28.2, BD Biosciences) at 1 μg/ml, in the presence of 20 U/ml IL-2 and with or without 20 ng/ml IL-12 (Stemcell, 78027). IL-2 was obtained through the AIDS Research and Reference Reagent Program, Division of AIDS, National Institute of Allergy and Infectious Diseases, National Institutes of Health. Tregs were plated at 20,000 cells per well. On day 4, Tregs were restimulated with 50 nM phorbol-12-myristate-13-acetate (MilliporeSigma) and 250 nM ionomycin (MilliporeSigma) for 4 hours in the presence of 10 μg/ml Brefeldin A (BD Biosciences). Intracellular staining was performed using the Foxp3 Staining Buffer Set (eBioscience) and the following staining mix: LIVE/DEAD Fixable Near-IR Dead Cell Stain kit (Invitrogen), αTIGIT (clone MBSA43, eBioscience), αCD226 (clone 11A8, Biolegend), αIFN-γ (clone 4S.B3, Invitrogen), αFoxp3 (clone 236A/E7, BD Bioscience), and αT-bet (clone 4B10, Invitrogen). Stained Tregs were washed and acquired on a BD Fortessa flow cytometer.

TIGIT agonists and small-molecule inhibitors. TIGIT stimulation was provided with an agonist αTIGIT antibody (clone 318.28.2.1, a gift from Bristol-Myers Squibb) plate-bound at 50 μg/ml. As an isotype control, we used α-mouse IgG1 (clone P3.6.2.8.1, eBiosciences). Alternatively, TIGIT was stimulated with Recombinant Human CD155 Fc Chimera Protein (R&D Systems, 9174-CD-050) plate-bound at 10 μg/ml. As isotype control, we used α-human IgG1 (MilliporeSigma, I5154-1MG).

The FoxO1 inhibitor AS1842856 (EMD Millipore) was used at 25 nM, and the SHIP-1 inhibitor 3AC (Merck Millipore) was used at 1 μM.

Analysis of phosphorylation by FACS. Sorted Tregs were rested in serum-free complete RPMI for 2 hours at 37°C, followed by incubation with αCD3 and αCD28 at 20 μg/ml for 20 minutes on ice. After washing, Tregs were resuspended at 4×10^6 cells/ml in ice-cold PBS, 2% FBS, and incubated with soluble Fc-CD155 or isotype control (10 μg/ml), AffiniPure $F(ab')_2$ Fragment Goat α-Mouse and α-Human (Jackson ImmunoResearch, 115-006-003 and 109-006-003, respectively), and IL-12 at 20 ng/ml and incubated at 37°C for the indicated time. Stimulation was stopped with an equal volume of BD Cytofix buffer (BD Biosciences, 554655), followed by a 20-minute incubation at 37°C. Fixed cells were stored overnight at –80°C. The next day, cells were permeabilized with ice-cold BD PhosphoFlow Perm buffer III (BD Biosciences, 558050) and stained with the polyclonal antibodies αSHIP-1 Tyr1020 (Bioss, bs-3398R), αAKT 1/2/3 Thr305/308/309 (Bioss, bs-5182R), and αFoxO1 Ser256 (Bioss, bs-3142R). After a 2-hour incubation at room temperature, cells were washed and acquired on a BD Fortessa flow cytometer.

Analysis of FoxO1 nuclear localization by immunofluorescence. 12-mm-diameter coverslips (VWR) were precoated with poly-L-lysine (0.02%, MilliporeSigma) for 20 minutes at room temperature, washed 3 times in water, and coated with αCD3, Fc-CD155, or isotype control for 4 hours at 37°C as described earlier.

To limit the number of fluorophores present on the surface of Tregs, for this experiment, magnetically isolated CD4 T cells were stained only with αCD25-PE-Cy7, and the top 2% of $CD25^{hi}$ cells was identified as Tregs. Sorted Tregs were rested in serum-free complete RPMI at 37°C for 2 hours and then seeded onto coated coverslips at a density of 100,000 cells/slip in complete RPMI with 5% human serum with soluble αCD28 (1 μg/ml) and IL-12 (20 ng/ml). An aliquot of Tregs was fixed directly at the end of the 2-hour serum starvation and identified as the unstimulated control.

After an overnight incubation at 37°C (~16 hours), cells were fixed with a solution of 4% paraformaldehyde in PBS and permeabilized with 0.3% Triton X-100. Coverslips were then blocked with PBS, 0.2% BSA, and stained overnight at 4°C with mouse αFoxP3-FITC (1:50, clone PCH101, eBioscience) and rabbit αFoxO1 (1:200, clone C29H4, Cell Signaling Technologies). The next day, coverslips were stained first with α-Rabbit polyclonal antibody Alexa Fluor 555 (1:200, Cell Signaling Technologies 07/2012) for 20 minutes at room temperature and then with DAPI 3 μM for 5 minutes at room temperature.

Cells were analyzed with a ×63 objective on a Leica SP8 confocal microscope. Two to three images per sample were acquired. Images were analyzed with Fiji (45) with a custom Java script that identifies the cytoplasmic and nuclear areas based on DAPI staining and calculates nuclear enrichment of normalized FoxO1 fluorescence.

Suppression assays. Tregs were preactivated to induce the Th1 phenotype as described earlier. Tregs were then washed, counted, and cocultured with freshly isolated Teffs that were previously stained with CellTrace CFSE (Invitrogen, C34554). Tregs and Teffs were cocultured at up to 40,000 total cells at Treg/Teff ratios ranging from 1:1 to 1:16, in the presence of 2 Treg Suppression Inspector beads per cell (Miltenyi, 130-092-909). After 4 days, cocultures were stained with LIVE/DEAD Fixable Near-IR, αIFN-γ, and αFoxp3 and acquired on a BD Fortessa flow cytometer.

CD226 gene deletion by CRISPR/Cas9. Tregs were seeded at a density of 5,000 cells/well and expanded in vitro with Dynabeads Human T-Activator CD3/CD28 (Thermo Fisher, 111.32D) at a ratio of 4 beads per cell in the presence of 100 U/ml of IL-2 in complete RPMI 1640 as described earlier. After 12–14 days, beads were removed magnetically, and Tregs were rested in the same media supplemented with IL-2 at a density of 100,000 cells/well. After 3 days, fresh beads were added to rested Tregs at a ratio of 1 bead per cell. After 2 days, beads were magnetically removed and Tregs were centrifugated and resuspended in Lonza electroporation buffer P3 at a concentration of 1×10^6 cells in 20 μl. Cells were then added to premixed guide RNAs (nontarget, GGTTCTTGACTACCGTAATT, and CD226 exon 3, ATCAATGGGCATCTTAACAC) and RNPs (1×10^6 cells per condition) and transferred to a 96-well electroporation cuvette plate. Electroporation was carried out using a Lonza 4D 96-well electroporation system with pulse code EH115. Immediately after electroporation, 80 μl prewarmed media was added to each well, and cells were rested for 15–60 minutes at 37°C. Cells were then moved to a conventional 96-well plate and stimulated to induce Th1 Tregs as described earlier, with the only difference that cell density was 100,000 cells/well.

Statistics. Flow cytometry data were analyzed using FlowJo v10.3.0. Figures and statistics were obtained using GraphPad Prism v7.0a. When comparing two conditions within the same individual we used paired 2-tailed *t* tests. For comparisons across 2 groups of unrelated individuals, we used unpaired 2-tailed *t* tests. When comparing 3 or more groups, we used ANOVA. When performing multiple paired 2-tailed *t* tests, we used Bonferroni's correction for multiple comparison. *P* values of 0.05 or less were considered significant. Data were presented as mean ± SEM, unless otherwise indicated.

Study approval. All subjects provided informed consent and approval was granted by the Institutional Review Board at Yale University. All experiments conformed to the principles of the WMA Declaration of Helsinki and the Department of Health and Human Services Belmont Report.

Author contributions

LEL designed the study, planned and performed experiments, analyzed data, and wrote the manuscript. PPA designed, performed, and analyzed CRISPR/Cas9 and microscopy experiments. ERS and NMN assisted with designing and performing experiments. MDV and DAH designed and supervised the study and wrote the manuscript.

Acknowledgments

The authors would like to thank Lesley Devine and Chao Wang for technical assistance with flow cytometry and the staff in the Yale-New Haven Hospital Multiple Sclerosis Center for help with patient recruit-

ment. This work was generously supported by grants from the National Institutes of Health (P01 AI045757, U19 AI046130, U19 AI070352, P01 AI073748 and P01 AI039671) and the Nancy Taylor Foundation for Chronic Diseases (to DAH). LEL is a fellow of the National Multiple Sclerosis Society (FG-1608-25643). DAH is also supported by grants from the National Institute of Neurological Disorders and Stroke and the Nancy Taylor Foundation for Chronic Diseases. The authors would also like to thank Tomokazu Sumida for insightful comments on the study and Jean-Marie Carpier for help with immunofluorescence analysis. We have received funding from Bristol-Myers Squibb to investigate TIGIT and other costimulatory pathways in patients with brain tumors.

Address correspondence to: Margarita Dominguez-Villar, Yale School of Medicine, Departments of Neurology and Immunobiology, 15 York Street, New Haven, Connecticut 06520, USA. Phone: 44.0.20.7594.3735; Email: m.dominguez-villar@imperial.ac.uk.

MDV's present address is: Department of Medicine, Imperial College London, London, United Kingdom.

1. Bennett CL, et al. The immune dysregulation, polyendocrinopathy, enteropathy, X-linked syndrome (IPEX) is caused by mutations of FOXP3. *Nat Genet*. 2001;27(1):20–21.
2. Baecher-Allan C, Hafler DA. Suppressor T cells in human diseases. *J Exp Med*. 2004;200(3):273–276.
3. Dominguez-Villar M, Hafler DA. Regulatory T cells in autoimmune disease. *Nat Immunol*. 2018;19(7):665–673.
4. Chaudhry A, et al. CD4+ regulatory T cells control TH17 responses in a Stat3-dependent manner. *Science*. 2009;326(5955):986–991.
5. Zheng Y, et al. Regulatory T-cell suppressor program co-opts transcription factor IRF4 to control T(H)2 responses. *Nature*. 2009;458(7236):351–356.
6. Koch MA, Tucker-Heard G, Perdue NR, Killebrew JR, Urdahl KB, Campbell DJ. The transcription factor T-bet controls regulatory T cell homeostasis and function during type 1 inflammation. *Nat Immunol*. 2009;10(6):595–602.
7. Koch MA, Thomas KR, Perdue NR, Smigiel KS, Srivastava S, Campbell DJ. T-bet(+) Treg cells undergo abortive Th1 cell differentiation due to impaired expression of IL-12 receptor β2. *Immunity*. 2012;37(3):501–510.
8. Dominguez-Villar M, Baecher-Allan CM, Hafler DA. Identification of T helper type 1-like, Foxp3+ regulatory T cells in human autoimmune disease. *Nat Med*. 2011;17(6):673–675.
9. McClymont SA, et al. Plasticity of human regulatory T cells in healthy subjects and patients with type 1 diabetes. *J Immunol*. 2011;186(7):3918–3926.
10. Arterbery AS, et al. Production of proinflammatory cytokines by monocytes in liver-transplanted recipients with de novo autoimmune hepatitis is enhanced and induces TH1-like regulatory T cells. *J Immunol*. 2016;196(10):4040–4051.
11. Cao AT, et al. TLR4 regulates IFN-γ and IL-17 production by both thymic and induced Foxp3+ Tregs during intestinal inflammation. *J Leukoc Biol*. 2014;96(5):895–905.
12. Feng T, Cao AT, Weaver CT, Elson CO, Cong Y. Interleukin-12 converts Foxp3+ regulatory T cells to interferon-γ-producing Foxp3+ T cells that inhibit colitis. *Gastroenterology*. 2011;140(7):2031–2043.
13. Hernandez AL, et al. Sodium chloride inhibits the suppressive function of FOXP3+ regulatory T cells. *J Clin Invest*. 2015;125(11):4212–4222.
14. Sumida T, et al. Activated β-catenin in Foxp3+ regulatory T cells links inflammatory environments to autoimmunity. *Nat Immunol*. 2018;19(12):1391–1402.
15. Kitz A, de Marcken M, Gautron AS, Mitrovic M, Hafler DA, Dominguez-Villar M. AKT isoforms modulate Th1-like Treg generation and function in human autoimmune disease. *EMBO Rep*. 2016;17(8):1169–1183.
16. Yu X, et al. The surface protein TIGIT suppresses T cell activation by promoting the generation of mature immunoregulatory dendritic cells. *Nat Immunol*. 2009;10(1):48–57.
17. Boles KS, et al. A novel molecular interaction for the adhesion of follicular CD4 T cells to follicular DC. *Eur J Immunol*. 2009;39(3):695–703.
18. Johnston RJ, et al. The immunoreceptor TIGIT regulates antitumor and antiviral CD8(+) T cell effector function. *Cancer Cell*. 2014;26(6):923–937.
19. Lozano E, Dominguez-Villar M, Kuchroo V, Hafler DA. The TIGIT/CD226 axis regulates human T cell function. *J Immunol*. 2012;188(8):3869–3875.
20. Liu S, et al. Recruitment of Grb2 and SHIP1 by the ITT-like motif of TIGIT suppresses granule polarization and cytotoxicity of NK cells. *Cell Death Differ*. 2013;20(3):456–464.
21. Joller N, et al. Treg cells expressing the coinhibitory molecule TIGIT selectively inhibit proinflammatory Th1 and Th17 cell responses. *Immunity*. 2014;40(4):569–581.
22. Fuhrman CA, et al. Divergent phenotypes of human regulatory T cells expressing the receptors TIGIT and CD226. *J Immunol*. 2015;195(1):145–155.
23. Hafler JP, et al. CD226 Gly307Ser association with multiple autoimmune diseases. *Genes Immun*. 2009;10(1):5–10.
24. Piédavent-Salomon M, et al. Multiple sclerosis associated genetic variants of CD226 impair regulatory T cell function. *Brain*. 2015;138(Pt 11):3263–3274.
25. Roth TL, et al. Reprogramming human T cell function and specificity with non-viral genome targeting. *Nature*. 2018;559(7714):405–409.
26. Ouyang W, et al. Novel Foxo1-dependent transcriptional programs control T(reg) cell function. *Nature*. 2012;491(7425):554–559.
27. Zhang X, et al. Phosphorylation of serine 256 suppresses transactivation by FKHR (FOXO1) by multiple mechanisms. Direct

and indirect effects on nuclear/cytoplasmic shuttling and DNA binding. *J Biol Chem*. 2002;277(47):45276–45284.
28. Sattler M, Verma S, Pride YB, Salgia R, Rohrschneider LR, Griffin JD. SHIP1, an SH2 domain containing polyinositol-5-phosphatase, regulates migration through two critical tyrosine residues and forms a novel signaling complex with DOK1 and CRKL. *J Biol Chem*. 2001;276(4):2451–2458.
29. Pauls SD, Marshall AJ. Regulation of immune cell signaling by SHIP1: A phosphatase, scaffold protein, and potential therapeutic target. *Eur J Immunol*. 2017;47(6):932–945.
30. Huynh A, et al. Control of PI(3) kinase in Treg cells maintains homeostasis and lineage stability. *Nat Immunol*. 2015;16(2):188–196.
31. Delgoffe GM, et al. Stability and function of regulatory T cells is maintained by a neuropilin-1-semaphorin-4a axis. *Nature*. 2013;501(7466):252–256.
32. Fourcade J, et al. CD226 opposes TIGIT to disrupt Tregs in melanoma. *JCI Insight*. 2018;3(14):e121157.
33. Zhang Z, Wu N, Lu Y, Davidson D, Colonna M, Veillette A. DNAM-1 controls NK cell activation via an ITT-like motif. *J Exp Med*. 2015;212(12):2165–2182.
34. Gaud G, et al. The costimulatory molecule CD226 signals through VAV1 to amplify TCR signals and promote IL-17 production by CD4+ T cells. *Sci Signal*. 2018;11(538):eaar3083.
35. Urbanellis P, et al. The regulatory T cell effector molecule fibrinogen-like protein 2 is necessary for the development of rapamycin-induced tolerance to fully MHC-mismatched murine cardiac allografts. *Immunology*. 2015;144(1):91–106.
36. Krahn AK, Ma K, Hou S, Duronio V, Marshall AJ. Two distinct waves of membrane-proximal B cell antigen receptor signaling differentially regulated by Src homology 2-containing inositol polyphosphate 5-phosphatase. *J Immunol*. 2004;172(1):331–339.
37. Luo CT, Liao W, Dadi S, Toure A, Li MO. Graded Foxo1 activity in Treg cells differentiates tumour immunity from spontaneous autoimmunity. *Nature*. 2016;529(7587):532–536.
38. Li XY, et al. CD155 loss enhances tumor suppression via combined host and tumor-intrinsic mechanisms. *J Clin Invest*. 2018;128(6):2613–2625.
39. Guillerey C, et al. TIGIT immune checkpoint blockade restores CD8+ T-cell immunity against multiple myeloma. *Blood*. 2018;132(16):1689–1694.
40. Gumbleton M, et al. Dual enhancement of T and NK cell function by pulsatile inhibition of SHIP1 improves antitumor immunity and survival. *Sci Signal*. 2017;10(500):eaam5353.
41. De Jager PL, et al. The role of the CD58 locus in multiple sclerosis. *Proc Natl Acad Sci USA*. 2009;106(13):5264–5269.
42. Dendrou CA, et al. Cell-specific protein phenotypes for the autoimmune locus IL2RA using a genotype-selectable human bioresource. *Nat Genet*. 2009;41(9):1011–1015.
43. Patsopoulos NA, et al. Genome-wide meta-analysis identifies novel multiple sclerosis susceptibility loci. *Ann Neurol*. 2011;70(6):897–912.
44. Dixon KO, et al. Functional Anti-TIGIT antibodies regulate development of autoimmunity and antitumor immunity. *J Immunol*. 2018;200(8):3000–3007.
45. Schindelin J, et al. Fiji: an open-source platform for biological-image analysis. *Nat Methods*. 2012;9(7):676–682.